Ann. N.Y. Acad. Sci. ISSN 0077-89

ANNALS OF THE NEW YORK ACADEMY OF SCIENCES
Special Issue: *Climate Sciences*
REVIEW

Perspectives of regional paleoclimate modeling

Patrick Ludwig,[1] Juan J. Gómez-Navarro,[2] Joaquim G. Pinto,[1] Christoph C. Raible,[3,4] Sebastian Wagner,[5] and Eduardo Zorita[5]

[1]Institute of Meteorology and Climate Research, Karlsruhe Institute of Technology, Karlsruhe, Germany. [2]Department of Physics, University of Murcia, Murcia, Spain. [3]Climate and Environmental Physics, University of Bern, Bern, Switzerland. [4]Oeschger Centre for Climate Change Research, University of Bern, Bern, Switzerland. [5]Institute of Coastal Research, Helmholtz-Zentrum Geesthacht, Geesthacht, Germany

Address for correspondence: Patrick Ludwig, Institute of Meteorology and Climate Research, Karlsruhe Institute of Technology, PO Box 3640 76021 Karlsruhe, Eggenstein-Leopoldshafen, Baden-Württemberg 76344, Germany. patrick.ludwig@kit.edu

Regional climate modeling bridges the gap between the coarse resolution of current global climate models and the regional-to-local scales, where the impacts of climate change are of primary interest. Here, we present a review of the added value of the regional climate modeling approach within the scope of paleoclimate research and discuss the current major challenges and perspectives. Two time periods serve as an example: the Holocene, including the Last Millennium, and the Last Glacial Maximum. Reviewing the existing literature reveals the benefits of regional paleo climate modeling, particularly over areas with complex terrain. However, this depends largely on the variable of interest, as the added value of regional modeling arises from a more realistic representation of physical processes and climate feedbacks compared to global climate models, and this affects different climate variables in various ways. In particular, hydrological processes have been shown to be better represented in regional models, and they can deliver more realistic meteorological data to drive ice sheet and glacier modeling. Thus, regional climate models provide a clear benefit to answer fundamental paleoclimate research questions and may be key to advance a meaningful joint interpretation of climate model and proxy data.

Keywords: proxy data; regional climate modeling; paleoclimate

Introduction

The effect of anthropogenic greenhouse gases on present and future climate has been firmly established through the analysis of observations and climate simulations with comprehensive earth system models (ESMs).[1] However, uncertainties remain, especially in the context of hydrological changes. In particular, the magnitude of the response of the global climate to alterations in the external climate forcing has not yet been constrained to a narrow scope of possible ranges. Further uncertainties arise at regional scales, as local processes introduce feedbacks that may either amplify or attenuate such global response, concerning both the mean climate state and the intensity and frequency of extreme events. The simulation of past climates, together with the analysis of the available indirect information encoded in biogeochemical archives, can help to assess and potentially reduce these uncertainties.[2,3] For example, Fischer *et al.* have recently used warm events of the past to illuminate the potential climate change and impacts in a warming world.[4] Thus, such past events can provide a real-world testbed to estimate the impact of different forcing in the climate system.

The evolution of past climates can be used to identify and understand underlying mechanisms of natural climate variability, as well as to evaluate climate models that are also used to project future climate change. For this purpose, an interplay between climate information derived from instrumental observations or indirect archives and models is needed. However, archives such as ice cores, tree

doi: 10.1111/nyas.13865

rings, and documents provide only limited paleoclimate information. These so-called proxy records may be sensitive to one or more physical variables (mostly temperature and hydrological changes) and can be used to reconstruct their evolution back in time on regional to local scales. In contrast, global climate models, such as general circulation models (GCMs) and ESMs, provide a more comprehensive and, in the respective virtual world of the model, physical consistent picture of past climates, despite the still existing uncertainties in the past boundary conditions. These global models are currently implemented with a relatively coarse spatial resolution (up to 1° in longitude and latitude) to reduce their computational cost, therefore enabling the simulation of long periods of past climates.[3,5] Thus, these coarse resolution simulations often lack a realistic representation of key processes at regional scales.

Given this mismatch in spatial resolution, several approaches have been pursued to compare proxy data with paleoclimate model simulations,[6,7] in order to evaluate the models and/or identify mechanisms explaining variations recorded by the proxy data.[8] A first approach consists of transforming (up-scaling) the local-to-regional climate proxy information to either large-scale averages,[9–11] or climate fields,[12,13] using statistical reconstruction methods. Second, climate model output can be downscaled using either statistical methods or proxy forward models. The latter generates synthetic proxy records, for example, the tree ring width,[14,15] using the large-scale variables provided by the climate model. Though being computationally efficient standard tools, both up-scaling and statistical downscaling approaches often suffer from multiple shortcomings, including (1) the short observational periods (50–150 years) for method calibration, (2) the sometimes questionable assumption of stationary, statistical links, and (3) the statistical degradation of the climate signal/variability.[16–18] A third approach, which is the focus of the present study, is referred to as dynamical downscaling. It consists of increasing the spatial resolution (horizontal and vertical) by producing a climate simulation for a regional subdomain of interest using a regional climate model (RCM). The advantage is that RCM simulations do not rely on statistical relationships, but explicitly resolve the physical processes relevant on the regional to local scales and thus are closer to the range of spatial representability of proxy data. However, model biases, either from the RCM itself or inherited by the driving global model, usually remain. The dynamical downscaling approach is commonly used in present day climate analysis and future climate projections.[19,20] The latter aims to provide better estimates of future climate change, for example, in impact studies and adaptation measures.[1,21,22] However, the application of RCMs in the paleoclimate context is less common. Reasons for this include the high computational costs (as for paleoclimate questions long-term simulations become necessary) and the limited availability of temporal highly resolved full 3D atmospheric fields from global model simulations, which are needed as periodic boundary conditions by the RCM. Additionally, technical issues such as the inclusion of external forcing (e.g., atmospheric composition, land use changes, etc.) emerge when setting up an RCM for paleoclimate conditions.

First attempts to use regional climate modeling in the historical and paleo context date back to the 2000s, with a first RCM simulation addressing the climate changes during the Younger Dryas period (about 12 ky ago).[23] After first global climate model simulations for the Last Millennium became available, Gómez-Navarro *et al.* downscaled these simulations for the Iberian Peninsula.[24] For studies encompassing entire Europe, evidence is provided of the benefit of using a more highly resolved RCM compared to the global model, in particular for precipitation.[25–27] Furthermore, some regional modeling studies focused on the Last Glacial Maximum (LGM)[28] defined as the time period of the maximum global land ice volume from 22 to 19 ky ago.[29,30] As illustrated in studies for the New Zealand Alps[31] and the Cordilleran ice sheet,[32] precipitation obtained from high-resolution LGM simulations is beneficial for mountain glacier modeling.

The aim of this study is to review the perspectives of regional climate modeling in the context of paleoclimate research. We first focus on the technical implementation and on issues of the dynamical downscaling approach for paleoclimate investigations. Then, the application of RCMs in the paleoperspective is reviewed in more detail for (1) the Holocene including the Last Millennium and (2) the LGM. Finally, future perspectives of regional paleoclimate modeling derived from our experience so far are presented.

Ann. N.Y. Acad. Sci. xxxx (2018) 1–16 © 2018 The Authors. *Annals of the New York Academy of Sciences* published by Wiley Periodicals, Inc. on behalf of New York Academy of Sciences.

Models and boundary conditions

An RCM is a regional variant of a global model applied to a limited area of interest and therefore allows for a considerably finer horizontal and vertical resolution compared to global models. This enables to explicitly resolve physical processes relevant on local scales that otherwise have to be parameterized in global models. Parametrizations are needed to consider additional processes that cannot be explicitly simulated by the global climate model. Some processes, like the simulation of convection, take place on a considerably finer scale that is sometimes orders of magnitude below the grid spacing of the global model. The parameterization tries to mimic this process by assessing the integrated effect of the large-scale state. However, this involves high uncertainties because of the crude approximation of the process using a simple parameterization.

To maintain the numerical stability and physical consistency of the model, a typical dynamical downscaling setup requires the use of multiple nesting steps, where the resolution should not increase with each step by more than a factor of three (Fig. 1). A standard resolution for present-day and future RCMs is 10–25 km,[22] and is increased to 1–3 km for specific applications.[33–37] For paleoclimate applications, the spatial resolution has usually been limited to about 50 km due to the demand of longer simulation periods, requiring a high amount of computational resources. Nevertheless, a spatial resolution of this order of magnitude is still more suitable for simulating precipitation extremes and the hydroclimate compared to global models.[38] Thus, the application of higher resolved RCMs could be considered as being generally beneficial when investigating climate extremes, also due to the fact that they can produce additional internal variability,[39] in contrast to an extension of the GCM/ESM ensemble size.

Technically, an RCM is driven at the boundaries by the data obtained from a global climate simulation or a global meteorological reanalysis product. The driving 3D fields comprise a number of meteorological variables including temperature, wind, humidity, or pressure, as well as 2D variables like surface pressure, surface temperature, sea-ice, or snow cover. In a standard setup, the RCM requires an initial field provided by the driving GCM, but otherwise it can freely generate its own meteorological fields in the interior of the domain in the subsequent simulation steps, only subject to the boundary conditions provided by the global simulations.

The coupling between the global model and RCM at the domain boundaries deserves some considerations, since it cannot always be guaranteed that all physical quantities, such as energy or water mass, enter or leave the model domain in a physically consistent way.[40] These spurious effects are caused by the sudden change in the horizontal and vertical resolution from the coarse global model grid to the higher resolved RCM grid, which is mathematically implemented through a so-called sponge zone.[41] The sponge zone includes a number of grid points (5–10) along the borders of the RCM domain, and is usually excluded from further analysis for not being physically consistent.

In addition to this classical setup with only boundary forcing, other approaches have been developed to drive the RCM by the global model. One of them is the spectral nudging approach, in which the individual variables (e.g., the horizontal wind components at mid- and upper levels) inside the RCM domain are nudged toward the large-scale atmospheric flow conditions as present in the coarser forcing data. Still, the RCM is free to simulate the smaller scale circulation independently, particularly at lower levels. A close similarity to the large-scale circulation between RCM and GCM is often desirable, for example, to avoid that the RCM develops its own internal large-scale variability. This is particularly the case when the RCM domain is large and not strongly constrained by the driving fields at its boundaries. For example, spectral nudging has recently been applied to hindcast and downscale global reanalysis products to spatial scales of 50 km to better mimic regional scale processes in the observational period.[42]

Numerous studies have been carried out to evaluate the added value of RCM simulations over raw GCM output by comparing the simulations with observational data for different regions and applications.[43–46] A general conclusion of those studies is that hydrological variables and near-surface winds usually show larger improvements than near-surface temperatures, especially over regions with complex terrain including coastal areas with a ragged shoreline.[24] Further, it has been demonstrated that even slight changes in the strength and structure of the large-scale

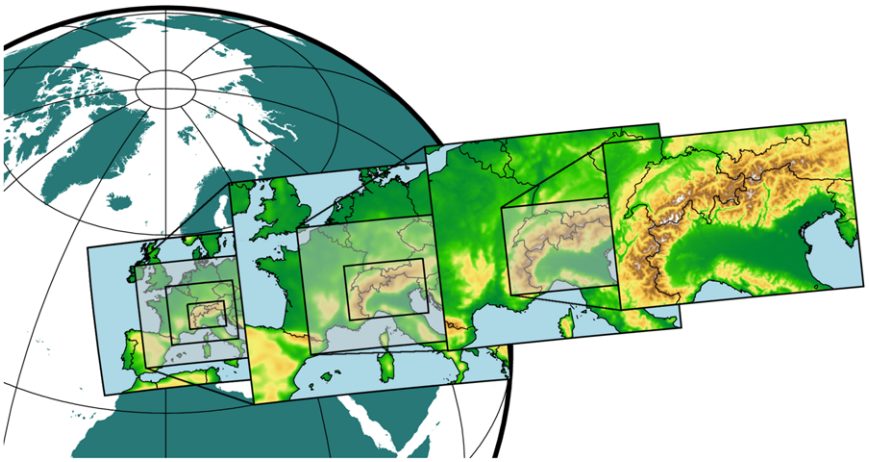

Figure 1. **From global to regional scales: a schematic of a typical nested domains setup in dynamical downscaling exercises. In this case, up to four domains have to be nested to downscale the GCM fields from a spatial resolution of 1° to the final target of 2 km over the Alpine region. In each step of the simulation, the RCM iteratively resolves the equations for each outer domain and uses this information to provide the boundary conditions to the interior one.**

atmospheric circulation, for instance, between reanalysis and GCM simulations, can have profound effects on the precipitation simulated by an RCM over the western parts of the Alpine region.[47]

As previously mentioned, the number of regional paleoclimate simulations is comparatively small compared to present-day and future climate impact studies. There are several—mostly technical—reasons that explain this situation. First, the general setup concerning the choice, selection, and implementation of external forcing must be as similar as possible to the driving GCM. This is not very demanding for some forcing agents, such as transient changes in greenhouse gas concentrations or slowly evolving changes on an interannual frequency as for orbital parameters, since routines for simulating the present-day and future climate already exist. For other important external forcing agents, such as changes in solar and volcanic activity, land use, the build-up of ice sheets, river routing or isostatic rebound, and different land-sea-mask, the technical requirements are more challenging because those routines usually need to be modified, adapted, or even newly developed to be used in an RCM. An example for different forcing for the Last Millennium is provided in Figure 2, representing changes of several important external forcing agents.

The uncertainties inherent in reconstructing external forcing are illustrated through prescribing different solar forcing estimates (Fig. 2). The changes in solar activity are reconstructed using indirect proxy records such as delta ^{13}C contained in trees or ^{10}Be contained in ice cores. These records are eventually linked to observed changes in solar activity starting in the 1970s of the 20th century. A significant uncertainty is the amplitude of the low-frequency variability in the solar activity.[48,49]

Volcanic activity (Fig. 2) is reconstructed from the acidity of ice layers in polar ice cores. The acidity is the remnant of past volcanic explosive eruptions that emit large amounts of sulfate aerosols into the upper troposphere and stratosphere, eventually deposited on the polar ice caps. The implementation of volcanic activity in RCM simulations is not straightforward. Volcanic activity can be implemented in present climate simulations when the emitted amount of sulfur and the eruption site are known. In paleoclimate simulations, this information is usually not completely available. The volcanic reconstructions used for global simulations are restricted to estimations of averages over latitudinal bands several tens of degrees wide, and are provided as simplified exponential vertical decay in the change of aerosol optical depth over time caused by a volcanic eruption.[50–52]

To represent volcanic activity in RCM simulations, an integrated perturbation of the incoming solar radiation at the top of the troposphere caused

Ann. N.Y. Acad. Sci. xxxx (2018) 1–16 © 2018 The Authors. *Annals of the New York Academy of Sciences* published by Wiley Periodicals, Inc. on behalf of New York Academy of Sciences.

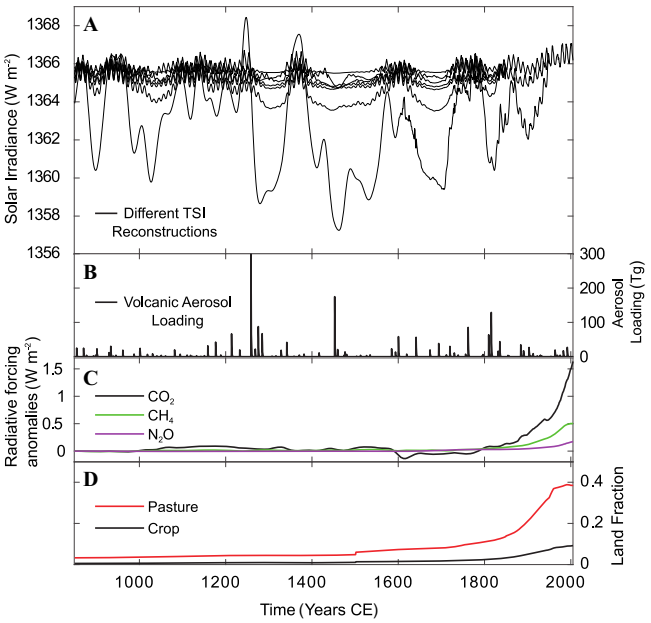

Figure 2. Forcing used for the Last Millennium simulations. From top to bottom: (A) Different total solar irradiance (TSI) reconstructions;[107] (B) example of a volcanic forcing as total volcanic aerosol mass; (C) radiative forcing (RF, calculated according to IPCC) from the greenhouse gases CO_2, CH_4, and N_2O;[108] (D) major changes in land cover (as fraction of global land area).[107]

by the volcanic eruption can be estimated. The perturbation of incoming solar radiation can be indirectly inferred from the diagnosis of the changes in shortwave radiation in the global simulation. These changes are then integrated into a so-called effective (transient) solar constant that is used in the solar routine of the RCM.[26]

The reconstruction of greenhouse gases concentrations in the atmosphere (Fig. 2) is based on the analysis of air bubbles trapped in ice cores.[49] The implementation into RCMs in the paleoclimate context is not as problematic, because routines used to represent recent and future climate change can be directly employed. In contrast, land use changes (Fig. 2) are more difficult to integrate into RCMs, because the schemes to represent land surface characteristics might be different in the driving GCM/ESM and in the RCM.[53] More specifically, changes in land use are represented the GCM/ESM by prescribing for each model grid cell a dominant plant functional type (forest, cropland, etc.), which is then translated in grid-cell averages of physically variables, for example, surface wind-drag. In an RCM, variables such as surface roughness length and albedo, vegetation fraction, and related quantities must be set to a reasonable value correspondent to the climate conditions in a certain region and a certain time period at the defined spatial resolution. Therefore, the land use prescribed in GCM simulations needs to be translated into variables that can be used within the RCM in a physically consistent way. This problem is exacerbated due to the different spatial resolution of the global and the regional models. The RCM requires information at a higher spatial resolution than provided by the global model, in particular in regions of complex terrain. Further, these parameters are normally kept constant in time in present-day simulations, so the model internal routines have to be adapted to allow temporal variations throughout the paleoclimate simulation.

The consideration of ice sheets and associated changes of the land-sea mask in the regional simulations relies on information from ice sheet models, which are currently working on global scales with a horizontal resolution of about 1° in both longitude and latitude.[54] The implementation of ice sheets is of particular importance for simulations of glacial conditions. Due to their large extent, ice sheets are able to influence the atmospheric circulation.[55] Thus, the application of RCMs to glacial periods demands a careful, and in the literature barely addressed, implementation of the available ice sheet and

land-sea-mask information as surface boundary conditions.[30]

The Holocene including the Last Millennium

One of the earliest studies using a transient GCM simulation of the Last Millennium is that of Gómez-Navarro *et al.*[24] The authors used an RCM over the Iberian Peninsula with a horizontal resolution of 30 km and concluded that the added value of the regional model is mainly found for the high-frequency (daily) variations, in particular for hydrological variables such as precipitation. A follow-up study confirmed and generalized these findings for the entire European continent.[25] The most prominent improvements pertain to a more realistic representation of the probability distribution of precipitation amounts on the regional scale, especially in regions with complex topography such as the Pyrenees and the Alpine region. The mean temperature is closely linked to changes in external forcing also on the (averaged) regional scale, whereas precipitation is primarily affected by modes of atmospheric internal variability such as the North Atlantic Oscillation.

In an additional study, the latter simulation has been compared with proxy-based reconstructions.[26] The main outcome is summarized in Figure 3, which shows the reconstructions of surface air temperature (SAT)[56] and precipitation,[57] together with the respective simulated variables for nine European subregions. In general, the simulated temperature variability in Northern Europe is larger than in Southern Europe. Likewise, the simulated winter variability in these areas is larger than in summer, which is also true for the proxy data. The temporal agreement between the simulation and proxy data is generally higher for winter and in Central Europe. A clear upward trend of SATs exists for all seasons and areas in the 20th century, which is larger in Northern Europe. Nevertheless, this upward trend sets in later in the reconstructions (around 1900) than in the simulation (1790–1810). For precipitation, differences between the RCM and the GCM are larger (not shown), as the precipitation processes are more strongly influenced by differences in the orography and the parametrizations used in the respective model. No significant temporal correlation between the reconstruction and the RCM simulation can be found (Fig. 3). The precipitation variability is larger in mountainous areas such as for the Alps, Turkey, or the Iberian Peninsula in both the RCM and the reconstruction. In contrast to the SAT, no seasonal or regional common trend exists for precipitation.

The physical consistency across different reconstructed variables has also been considered.[26] The authors showed how the RCM realistically reproduces the linkage between leading modes of mean sea-level pressure, temperature, and precipitation variability observed in the real climate, a connection that is weaker or even missing in the reconstructions. This allowed the authors to hint at the existence of potential inconsistencies in proxy archives of different variables.

Further studies applied RCMs to other regions. One example is the Baltic Sea area, where the authors investigated the influence of deforestation on the climate over Northern Europe for time slices of the mid-Holocene and the preindustrial period.[58] The results show a clear impact of the different vegetation patterns on the local climate, not only over northern Europe but also over remote areas such as the Mediterranean. This is caused by spatially varying mechanisms related to albedo changes, leading to a cooling in southern Europe and a warming in central and Eastern Europe induced by a reduction in evapotranspiration over deforested areas.

On the longer, Holocene, time scale, Russo and Cubasch analyzed time slice simulations over Europe.[59] In contrast to the Last Millennium, when the external forcing is dominated by solar variations and volcanic eruptions and to a certain degree by land use changes, differences between the mid-Holocene and the late Holocene are characterized by changes in Earth's orbital parameters. Those orbital parameters influence the seasonal distribution of incoming solar insolation. By comparing these data to a pollen-based data set, the improvement by dynamical downscaling could be demonstrated compared to the raw GCM output.[59,60]

Reaching back to the period of the Younger Dryas (12 ky ago), a regional model with 50 km horizontal resolution has been used for time slice simulations over the European Mediterranean region and Northern Africa including different combinations of external forcing.[61] In general, a drying trend in the regional domain is found, accompanied by a decrease in the amplitude of intra-annual temperature variability. Specifically, the authors

Ann. N.Y. Acad. Sci. xxxx (2018) 1–16 © 2018 The Authors. *Annals of the New York Academy of Sciences* published by Wiley Periodicals, Inc. on behalf of New York Academy of Sciences.

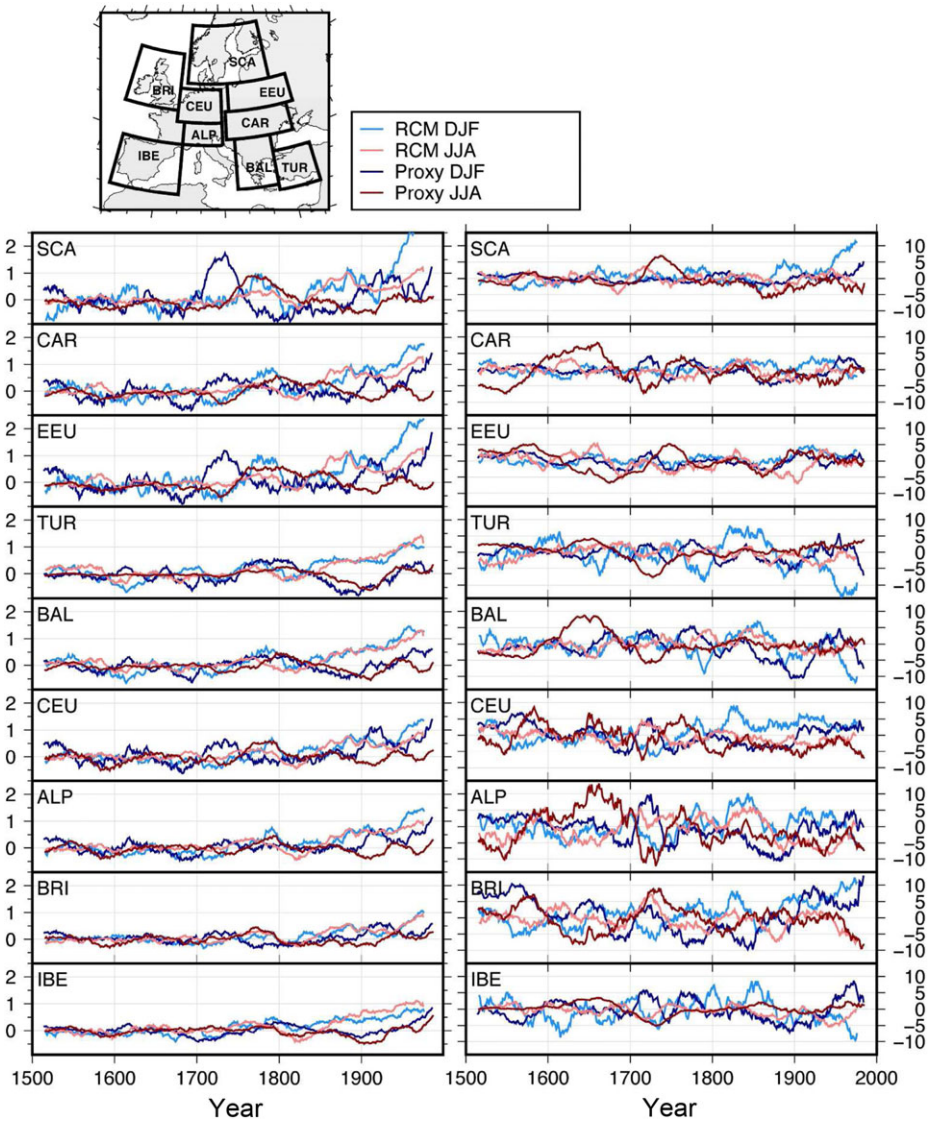

Figure 3. Thirty-one-year running mean of surface air temperature (K) (SAT, left) and precipitation (mm/month) (right) anomaly series averaged for the nine subregions defined in the map on top. In all cases, light and dark colors represent the model output and the reconstruction, respectively. All series depict anomalies respect to the preindustrial period (1500–1850).

noted that the regional simulation indicates some considerable spatial hydrological contrasts that are not evident in the GCM for subregions over the Mediterranean, challenging some of earlier hypotheses based on the interpretation of archaeological, palynological, and geomorphological evidence.[62]

For continents other than Europe, few studies exist in the paleoclimate context of the last millennium and the Holocene, despite the wealth of proxy records in these regions. This is especially remarkable as many other continental areas such as the Americas and eastern Asia are characterized by complex terrain (American Cordillera and Himalayan Mountains). Available studies mostly focus on changes in mid-Holocene climate for North America,[63] Western Africa,[64] Iran,[65] and China,[66] but also on changes between present-day and preindustrial periods for southern South America.[67] For the Tibetan Plateau, the natural

variability in the Earth's climate system in response to tectonic processes and global climate change during the LGM mid-Holocene has been analyzed.[68] In addition, monsoon changes have been investigated in a regional simulation for over eastern Asia,[69] and regional simulations for New Zealand with different prescribed sea surface temperature (SST) fields have been analyzed to test the sensitivity of the lower boundary forcing.[70]

The Last Glacial Maximum

The LGM (21 ky ago)[28] provides another excellent opportunity for testing climate models under boundary conditions different from present day. This is the case, for example, in the third, or more recently fourth phase of the Paleoclimate Modelling Intercomparison Project (PMIP).[3,71] However, the number of RCM applications under LGM conditions is rather limited compared to the number of GCM studies.

The adaption of RCMs to the changed LGM boundary conditions first needs to overcome some technical issues. Among them are the consideration of changes of the orbital parameters (Fig. 4A), changes in the greenhouse gas concentrations (e.g., CO_2, Fig. 4A), the implementation of ice sheets, and the associated drop in sea level that caused changes to the land-sea mask (Fig. 4B). Here, we interpolated the ice sheets and land-sea-mask data as given by the PMIP3 21ka experimental design onto the RCM grid.[72] Another critical point is the incorporation of land use changes into RCMs, since only a few global land use/vegetation reconstructions are available for LGM conditions.[73,74] Of particular importance is the synergy between the climate model and proxy data, since proxy data are needed on the one hand to reconstruct the glacial boundary conditions and on the other hand to validate the RCM simulations.

In a recent application, the regional weather research and forecasting (WRF) model was adapted to LGM boundary conditions and 30-year time slices were simulated.[30] The authors showed some added value of the RCM compared to the driving GCM simulation. This is illustrated in Figure 5 where the simulated RCM precipitation fields show a distinct higher spatial variability compared to their GCM counterpart. A comparison to reconstructions based on pollen data (Fig. 5E) also reveals a clear benefit of employing the RCM that offers a higher spatial resolution (Fig. 5F and G).[75] A further improvement of the glacial climate, particularly in Western Europe, is achieved when prescribing the North Atlantic SSTs according to reconstructions. In this case, the RCM is able to simulate the southern permafrost margin[76] much more realistically than the GCM.[30] Much effort is currently underway to improve this interpretation and refine field data for the LGM permafrost extent.[77] Thus, the simulated permafrost distribution is an additional convincing example for the benefit of the higher resolution output of RCMs.

Earlier studies also discussed the added value of RCM simulations under LGM conditions over Europe.[29,78] Strandberg *et al.* performed a downscaling with an RCM in combination with a dynamic vegetation model to obtain vegetation that is consistent with the RCM climate.[29] Their results indicate that the simulated climate is sensitive to changes in vegetation, with a similar average model-proxy error for summer and winter. Furthermore, the RCM results are within the uncertainty limits of the proxy reconstructions for winter. This is similar to the results by Jost *et al.*, where the RCM simulated temperature fields are in much better agreement with paleodata than the driving GCM fields, particularly for the coldest month.[78] However, the good agreement for temperature is at the expense of the precipitation, which is overestimated along the western coasts of Europe and the Mediterranean compared to proxy evidence. Jost *et al.* discussed possible reasons for the overestimate: (1) too warm SSTs compared to the overlying air (as shown in Ref. 30), (2) different ice sheet reconstructions that lead to altered atmospheric circulation patterns (see Ref. 79), (3) lack of accurate vegetation reconstruction (see Ref. 29 regarding the sensitivity of vegetation), and (4) the role of permafrost.[78] As permafrost affects the soil hydrology by generating high soil moisture, it has a strong impact on the near SAT.

Regional modeling was also used to assess LGM climate for North America, focusing on the region close to the Laurentide Ice Sheet (LIS).[80,81] The LGM summer climate as simulated by the RCM is characterized by a strong low-level thermal gradient (maintained by the nearby cold LIS and the relatively warm land surface) along the southern margin of the LIS.[81] This zone of enhanced baroclinicity favors the development of cyclones

Ann. N.Y. Acad. Sci. xxxx (2018) 1–16 © 2018 The Authors. *Annals of the New York Academy of Sciences* published by Wiley Periodicals, Inc. on behalf of New York Academy of Sciences.

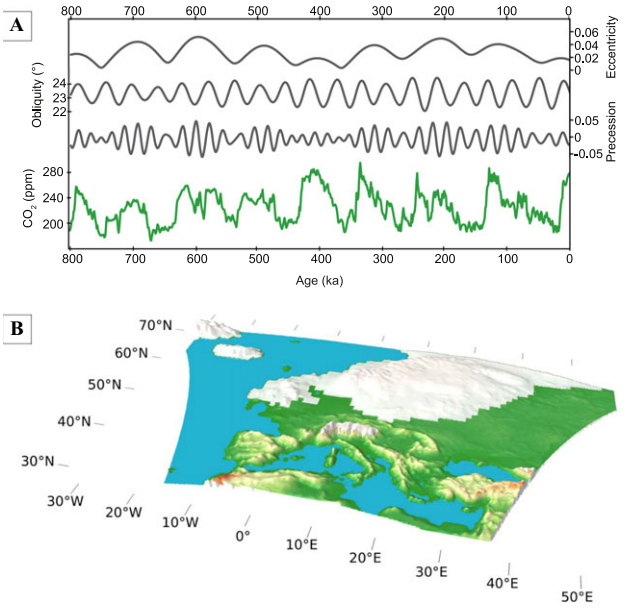

Figure 4. **(A) Orbital parameters over the past 800 ky and atmospheric concentration of CO_2 from Antarctic ice cores (adapted from IPCC 2013, fig. 5.3).[1] (B) RCM domain adapted to LGM surface boundary conditions (land-sea-mask and ice-sheets based on PMIP3 21Ka experimental design).[72]**

that move along the southern ice sheet margin. These cyclones produce strong, but infrequent northwesterly winds that help to interpret the observed distribution of loess depositions in the Great Plains.[81] The importance of loess as a climate proxy is discussed in additional studies.[82,83] For the LGM winter climate, the RCM produces a substantially different atmospheric response to the LGM boundary conditions than obtained by GCM simulation.[80] The RCM generates a split of the upper level flow around the blocking cyclone over the LIS that is primarily due to mechanical forcing by the LIS. The RCM results are in general agreement with proxy data. Unlike the GCM data, the RCM results are consistent with proxy information particularly over the Canadian High Arctic and thus may help to resolve discrepancies between proxy data and previous GCM simulations of the LGM climate.[80]

Similarly, for other regions, where the application of RCMs shows benefits when compared to the driving GCM, Ju *et al.* found a better agreement of the RCM simulated climate with geological reconstructions over East Asia.[84] In particular, for mideastern and southern China, the simulated GCM warming disagrees with cooling in paleodata, whereas the RCM reproduces a realistic cooler LGM climate. Another study focusing on the East Asian monsoon shows some improvements of the representation of the strengthening of the Asian winter and shrinking of the Asian summer monsoon by the RCM, which is closer to geological data than the GCM simulations.[85] For the South American monsoon under LGM conditions, the results from an RCM simulation are superior to those available from GCMs.[86] Here, the GCM did not realistically resolve the topography and regional-scale features of the South American climate. For New Zealand, Drost *et al.* compared an RCM simulation with proxy reconstructions.[87] The LGM cooling is indicated by the existence, or the lack of certain vegetation types (limited forest growth) in the reconstructions. However, the simulated cooling seems to be too low to explain the lack of forests, but the simulated regional LGM climate was much harsher, with stronger seasonality in temperature and winds and the addition of strong southerly polar wind intrusions. The authors concluded that not the absolute cooling, but the increase in extremes may have determined the absence of certain vegetation types.

Perspectives

We have presented examples of how regional climate modeling can provide a clear benefit compared to

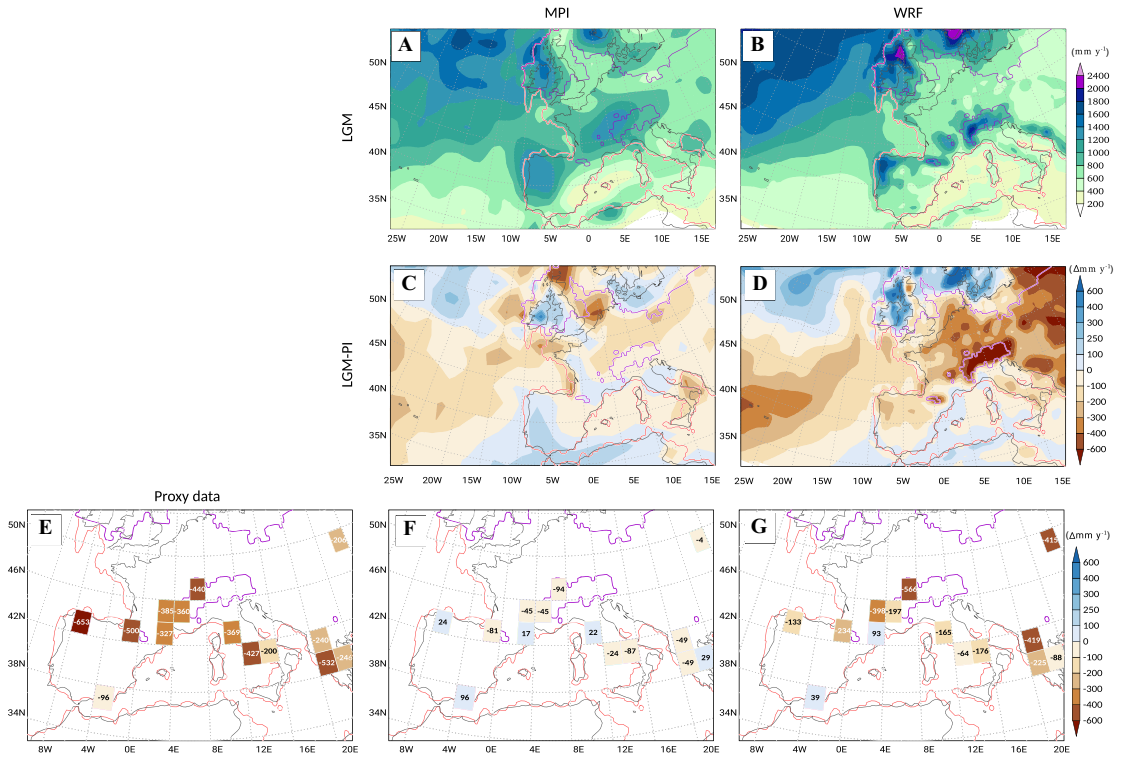

Figure 5. Simulated annual average GCM/RCM precipitation amount for LGM conditions and comparison of precipitation differences between LGM and preindustrial climate conditions based on proxy data: simulated precipitation (mm y^{-1}) (A) for MPI-ESM-P and (B) for WRF. Precipitation differences (Δmm y^{-1}) between corresponding LGM and PI simulations (C) for MPI-ESM-P and (D) for WRF. (E) Pollen-based precipitation difference (Δmm y^{-1}) between LGM and PI.[75] (F) and (G) as (C) and (D) but precipitation differences interpolated on proxy data grid (adapted from Ludwig *et al.*).[30]

global models to tackle fundamental paleoclimate research questions. While we largely focused on the Holocene, including the Last Millennium, and the LGM, the methods can theoretically be applied and extended to other periods. Given the higher spatial resolution of the RCM, the mesoscale circulation processes and interactions with other components of the climate system can better represented than in a GCM. Furthermore, the higher spatial resolution of the RCMs matches better the spatial representability of proxy data and provides a better platform for the comparison of climate model and proxy data. The enhanced resolution of (complex) terrain by the RCM is highly important, as proxy records are often retrieved from high altitudes, where the most sensitive climate archives (e.g., trees and ice cores) are found (Fig. 6 for a schematic of model–proxy comparison). However, still a certain (minimum) accuracy in the simulation of the mean atmospheric circulation is of ultimate importance to simulate atmospheric circulation patterns that are consistent with the lateral boundary conditions provided by the GCM. This includes, for example, characteristics like blocking frequency or the mean strength of the westerly circulation

In our view, three points have to be considered when specifying a scientific question for model–data comparison: (1) the region, (2) the variable under consideration, and (3) whether or not a higher resolution RCM can be effective from a cost/benefit point of view. For hydrological variables, the literature suggests that a better representation of the physical processes associated with the generation of precipitation provides more realistic distribution functions compared to the raw GCM/ESM model output, and this is particularly beneficial in areas with complex terrain.[22] A better treatment of such processes, including water vapor transport, is particularly beneficial for ice sheet and glacier modeling.[31,32] Concerning large-scale temperature,

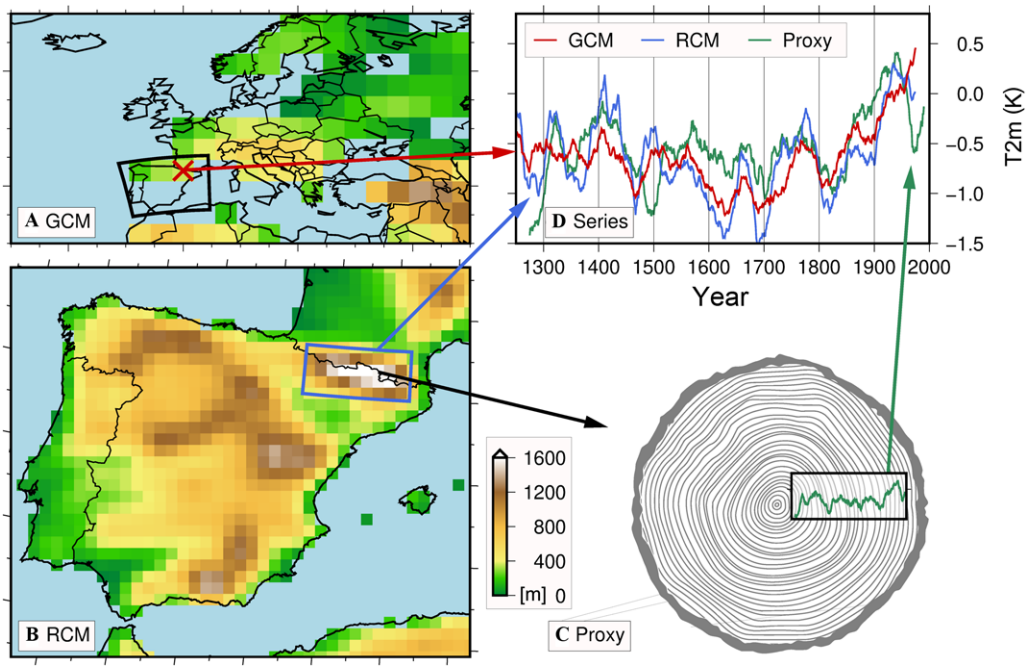

Figure 6. Schematic of GCM/RCM—proxy data comparison for temperature in the Pyrenees: (A) part of the GCM model domain (orography shaded), black box marks RCM domain, red cross marks grid point for time series data in (D); (B) RCM model domain (orography shaded), blue box marks area averaged over the Pyrenees for RCM data in (D), black arrow illustrates location of (C) tree ring used as proxy. (D) Synopsis of GCM, RCM, and proxy data time series.

this effect might be not so evident, because the RCM is strongly influenced by the driving GCM/ESM through the domain boundaries. The near-surface temperature has also a wide spatial correlation, typically of the order up to several hundreds of km, which is in contrast to precipitation (of the order of tens of kilometers). The correlation distance for precipitation is especially short in areas of complex terrain, for example, Norway, the Alpine region, and the Pyrenees. Furthermore, these regions include a wealth of temporally highly resolved proxy data (e.g., tree rings), thus attributing the added value of RCM simulations for model-data comparisons, as they might be used to better understand the physical linkages between the large-scale and local-scale climate at the proxy site.

Another important point is that proxies do not always record the mean temperature or precipitation (hydrological) averages over long time periods, but may rather be sensitive to extremes.[88] In spite of its relevance, the paleoclimate community has only marginally considered this issue. Given its better representation of the orography, mesoscale processes, and the ability to produce additional internal variability, RCMs can be particularly helpful to simulate past local extremes, thus enabling a better comparison to climate and/or historical proxies sensitive to such extremes.[39,89,90] While this principle is already well established for recent past and future climate, the new generation of convective permitting RCMs may open new research possibilities also with the scope of past climate change.[34]

An issue complicating the numerical coupling between the GCM and RCM is the lower boundary SST forcing over oceanic and/or coastal areas. Simply using the SST simulated by the GCM has the drawback that it does not take into account the intracell variability in thermal, hydrological, and topographical details of the underlying surface. Especially in coastal areas with complex terrain, affected by strong currents and tides, this can lead to additional biases.[91] These shortcomings can be avoided by employing coupled regional ESMs, which incorporate not only the atmosphere but also several other components of the climate system.[92–95] In particular, the coupling to a (regional or global)

dynamical ocean is important to represent the air–sea feedbacks.[96] This will also provide a better basis for improved model–proxy comparisons, particularly for continental shelf areas, where many maritime proxies are available.

The forward-modeling of proxy data can clearly benefit from the higher resolution of regional paleoclimate modeling.[97,98] So far, the standard approach is to reconstruct past climates from proxy archives using statistical methods by inverse modeling, and then compare these reconstructions with climate simulations. The complementary approach is forward-modeling: to simulate a synthetic proxy record (e.g., tree rings and isotopes) from the output of climate simulations, and then compare the synthetic with the real record.[14,15] For this kind of forward-modeling of proxy records, a realistic model of the proxy is required, which is certainly a bottleneck. Some type of proxy forward models may require only seasonal means of meteorological variables as input, but other types, such as oxygen stable isotopes in ice cores, require a full incorporation of an isotope enabled module in the climate model.[99] This requires in turn the driving fields (e.g., isotope concentrations at the model boundaries) that have to be provided by the global model. Despite the technical complexity, this approach is in general more accurate, in particular when the link between the proxy record and climate is strongly nonlinear or strongly depends on the background climate state. For these cases, a simple statistical calibration of the proxy record to reconstruct past climate states becomes more inaccurate.

In addition, forward-modeling of proxies complements another application of paleoclimate simulations, namely, the testing of climate field reconstruction methods.[100] These statistical methods aim to produce not only reconstructions of local climate based on proxy-records, but rather a full large-scale reconstruction combining a network of widely distributed records. In principle, these statistical methods can only be tested against observations in the 20th century. Another complementary strategy—termed pseudoproxy experiments—uses climate simulation as a virtual reality where the target climate fields are known.[2,17] The hurdle in these types of numerical experiments is that climate simulations do not produce proxy records. These have been so far statistically generated, preserving the statistical properties of real proxy records, but certainly, a more realistic way is to simulate these records using a physical- or biological-based model.

Another promising novel path of research is the consideration of proxy data assimilation.[101,102] The expectation is that such approaches can be used to improve the climate field reconstructions given the integration of the information from proxy observations in the high-resolution paleoclimate simulations.

Forthcoming regional paleoclimate simulations may also take advantage of new developments of climate models using different paradigms, for instance, including an unstructured icosahedral-triangular grid as in the icosahedral nonhydrostatic (ICON) model.[103,104] The use of a triangular grid helps to overcome the problem at the poles induced by the convergence of meridians in regular-grid models. With this structure, it would also be possible to represent certain regions of interest with considerably higher resolution in both nested and nonnested versions. The clear advantage of this approach is that no different external forcing agents outlined previously need to be adapted to the regional domain. Additionally, some of the boundary problems in the sponge zone between the GCM and the RCM are not as profound compared to a classical GCM–RCM downscaling setup. Given the more efficient use of computing time, this will enable the execution of additional ensemble experiments.

Lastly, the application of RCM perfectly fits into some of the goals of PMIP4, which will provide a better understanding of the climate system responses to different forcing and feedbacks.[3] In this project, the modeling groups will focus their efforts on five historical periods in Earth's history, including the last Millennium, mid-Holocene, and LGM. Another large initiative is the German paleoclimate modeling project PALMOD, which aims at modeling the last full glacial cycle (~135 K years) with an ESM.[105] Certainly, this project will provide an excellent basis for a better understanding of the climate processes associated with climate variability and change at different time scales and deliver a consistent basis for model–proxy comparison over very long-time periods. Further efforts for a coordinated model-data comparison will also be tackled by the PALEOLINK working group, associated with the PAGES 2k network.[106] In these and other endeavors, RCMs can become an important cornerstone to bridge the spatial scales, thus enabling

an effective and improved model comparison and validation.

Acknowledgments

J.J.G.N. acknowledges the CARM for the funding provided through the Seneca Foundation (project 20022/SF/16). J.G.P. thanks the AXA Research Fund for support. P.L., J.G.P., S.W., and E.Z. acknowledge partial funding from PALMOD. C.C.R. is supported by the Swiss National Science Foundation (grant: 200021_16244). We thank the two anonymous reviewers whose comments improved the manuscript. The authors additionally acknowledge support for the PALEOLINK project by the PAGES 2k Network coordinators. For more technical details on how to implement modified boundary conditions, please contact the corresponding author and the PALEOLINK project.

Competing interests

The authors declare no competing interests.

References

1. Bindoff, N.L., P.A. Stott, K.M. AchutaRao, *et al.* 2013. Detection and Attribution of Climate Change: from Global to Regional. In *Climate Change 2013: The Physical Science Basis. Contribution of Working Group I to the Fifth Assessment Report of the Intergovernmental Panel on Climate Change.* T.F. Stocker, D. Qin, G.-K. Plattner, *et al.*, Eds.: 86. Cambridge, UK and New York, NY: Cambridge University Press.
2. Harrison, S.P., P.J. Bartlein, K. Izumi, *et al.* 2015. Evaluation of CMIP5 palaeo-simulations to improve climate projections. *Nat. Clim. Change* **5:** 735–743.
3. Kageyama, M., P. Braconnot, S.P. Harrison, *et al.* 2016. PMIP4–CMIP6: the contribution of the Paleoclimate Modelling Intercomparison Project to CMIP6. *Geosci. Model Dev. Discuss.* **11:** 1033–1057.
4. Fischer, H. *et al.* 2018. Palaeoclimate constraints on a world with post-industrial warming of 2 degrees and beyond. *Nat. Geosci.* In press.
5. Jungclaus, J.H., E. Bard, M. Baroni, *et al.* 2017. The PMIP4 contribution to CMIP6—part 3: the last millennium, scientific objective, and experimental design for the PMIP4 past1000 simulations. *Geosci. Model Dev.* **10:** 4005–4033.
6. Bothe, O., M. Evans, L.F. Donado, *et al.* 2015. Continental-scale temperature variability in PMIP3 simulations and PAGES 2k regional temperature reconstructions over the past millennium. *Clim. Past* **11:** 1673–1699.
7. Smerdon, J.E., J. Luterbacher, S.J. Phipps, *et al.* 2017. Comparing proxy and model estimates of hydroclimate variability and change over the Common Era. *Clim. Past* **13:** 1851–1900.
8. Lehner, F., A. Born, C.C. Raible & T.F. Stocker. 2013. Amplified inception of European Little Ice Age by sea ice–ocean–atmosphere feedbacks. *J. Clim.* **26:** 7586–7602.
9. Ortega, P., F. Lehner, D. Swingedouw, *et al.* 2015. A model-tested North Atlantic Oscillation reconstruction for the past millennium. *Nature* **523:** 71–74.
10. PAGES 2k Consortium. 2013. Continental-scale temperature variability during the past two millennia. *Nat. Geosci.* **6:** 339–346.
11. PAGES 2k Consortium. 2017. A global multiproxy database for temperature reconstructions of the Common Era. *Sci. Data* **4:** 170088.
12. Jones, P.D. & M.E. Mann. 2004. Climate over past millennia. *Rev. Geophys.* **42:** RG2002.
13. Casty, C., C.C. Raible, T.F. Stocker, *et al.* 2007. A European pattern climatology 1766–2000. *Clim. Dyn.* **29:** 791–805.
14. Evans, M.N., B.K. Reichert, A. Kaplan, *et al.* 2006. A forward modeling approach to paleoclimatic interpretation of tree-ring data. *J. Geophys. Res. Biogeosci.* **111:** G03008.
15. Evans, M.N., S.E. Tolwinski-Ward, D.M. Thompson & K.J. Anchukaitis. 2013. Applications of proxy system modeling in high resolution paleoclimatology. *Quat. Sci. Rev.* **76:** 16–28.
16. Riedwyl, N., M. Küttel, J. Luterbacher & H. Wanner. 2009. Comparison of climate field reconstruction techniques: application to Europe. *Clim. Dyn.* **32:** 381–395.
17. Smerdon, J.E. 2012. Climate models as a test bed for climate reconstruction methods: pseudoproxy experiments. *Wiley Interdiscip. Rev. Clim. Change* **3:** 63–77.
18. Pinto, J.G. & C.C. Raible. 2012. Past and recent changes in the North Atlantic oscillation. *Wiley Interdiscip. Rev. Clim. Change* **3:** 79–90.
19. Jacob, D., L. Bärring, O.B. Christensen, *et al.* 2007. An inter-comparison of regional climate models for Europe: model performance in present-day climate. *Clim. Change* **81:** 31–52.
20. Vautard, R., A. Gobiet, D. Jacob, *et al.* 2013. The simulation of European heat waves from an ensemble of regional climate models within the EURO-CORDEX project. *Clim. Dyn.* **41:** 2555–2575.
21. Held, H., F.-W. Gerstengarbe, T. Pardowitz, *et al.* 2013. Projections of global warming-induced impacts on winter storm losses in the German private household sector. *Clim. Change* **121:** 195–207.
22. Jacob, D., J. Petersen, B. Eggert, *et al.* 2014. EURO-CORDEX: new high-resolution climate change projections for European impact research. *Reg. Environ. Change* **14:** 563–578.
23. Renssen, H., R.F.B. Isarin, D. Jacob, *et al.* 2001. Simulation of the Younger Dryas climate in Europe using a regional climate model nested in an AGCM: preliminary results. *Glob. Planet. Change* **30:** 41–57.
24. Gómez-Navarro, J.J., J.P. Montávez, S. Jerez, *et al.* 2011. A regional climate simulation over the Iberian Peninsula for the last millennium. *Clim. Past* **7:** 451–472.
25. Gómez-Navarro, J.J., J.P. Montávez, S. Wagner & E. Zorita. 2013. A regional climate palaeosimulation for Europe in the period 1500–1990—part 1: model validation. *Clim. Past* **9:** 1667–1682.

26. Gómez-Navarro, J.J., O. Bothe, S. Wagner, *et al.* 2015. A regional climate palaeosimulation for Europe in the period 1500–1990—part 2: shortcomings and strengths of models and reconstructions. *Clim. Past* **11:** 1077–1095.
27. Raible, C.C., O. Bärenbold & J.J. Gómez-navarro. 2017. Drought indices revisited–improving and testing of drought indices in a simulation of the last two millennia for Europe. *Tellus A Dyn. Meteorol. Oceanogr.* **69:** 1287492.
28. Yokoyama, Y., K. Lambeck, P. De Deckker, *et al.* 2000. Timing of the Last Glacial Maximum from observed sea-level minima. *Nature* **406:** 713–716.
29. Strandberg, G., J. Brandefelt, E. Kjellström & B. Smith. 2011. High-resolution regional simulation of last glacial maximum climate in Europe. *Tellus A Dyn. Meteorol. Oceanogr.* **63:** 107–125.
30. Ludwig, P., J.G. Pinto, C.C. Raible & Y. Shao. 2017. Impacts of surface boundary conditions on regional climate model simulations of European climate during the Last Glacial Maximum. *Geophys. Res. Lett.* **44:** 5086–5095.
31. Golledge, N.R., A.N. Mackintosh, B.M. Anderson, *et al.* 2012. Last Glacial Maximum climate in New Zealand inferred from a modelled Southern Alps icefield. *Quat. Sci. Rev.* **46:** 30–45.
32. Seguinot, J., C. Khroulev, I. Rogozhina, *et al.* 2014. The effect of climate forcing on numerical simulations of the Cordilleran ice sheet at the Last Glacial Maximum. *Cryosphere* **8:** 1087–1103.
33. Gómez-Navarro, J.J., C.C. Raible & S. Dierer. 2015. Sensitivity of the WRF model to PBL parametrisations and nesting techniques: evaluation of wind storms over complex terrain. *Geosci. Model Dev.* **8:** 3349–3363.
34. Leutwyler, D., O. Fuhrer, X. Lapillonne, *et al.* 2016. Towards European-scale convection-resolving climate simulations with GPUs: a study with COSMO 4.19. *Geosci. Model Dev.* **9:** 3393–3412.
35. Hackenbruch, J., G. Schädler & J.W. Schipper. 2016. Added value of high-resolution regional climate simulations for regional impact studies. *Meteorol. Zeitschrift* **25:** 291–304.
36. Messmer, M., J.J. Gómez-Navarro & C.C. Raible. 2017. Sensitivity experiments on the response of Vb cyclones to sea surface temperature and soil moisture changes. *Earth Syst. Dyn.* **8:** 477–493.
37. Gómez-Navarro, J.J., C.C. Raible, D. Bozhinova, *et al.* 2018. A new region-aware bias correction method for simulated precipitation in the Alpine region. *Geosci. Model Dev. Discuss.* https://doi.org/10.5194/gmd-2017-329.
38. Flato, G., J. Marotzke, B. Abiodun, *et al.* 2013. Evaluation of climate models. In *Climate Change 2013: The Physical Science Basis. Contribution of Working Group I to the Fifth Assessment Report of the Intergovernmental Panel on Climate Change*. T.F. Stocker, D. Qin, G.-K. Plattner, *et al.*, Eds.: 126. Cambridge, UK and New York, NY: Cambridge University Press.
39. Whan, K., F. Zwiers & J. Sillmann. 2016. The influence of atmospheric blocking on extreme winter minimum temperatures in North America. *J. Clim.* **29:** 4361–4381.
40. Marbaix, P., H. Gallée, O. Brasseur & J.-P. van Ypersele. 2003. Lateral boundary conditions in regional climate models: a detailed study of the relaxation procedure. *Mon. Weather Rev.* **131:** 461–479.
41. Davies, H.C. 1976. A laterul boundary formulation for multi-level prediction models. *Q. J. R. Meteorol. Soc.* **102:** 405–418.
42. Schubert-Frisius, M., F. Feser, H. von Storch & S. Rast. 2017. Optimal spectral nudging for global dynamic downscaling. *Mon. Weather Rev.* **145:** 909–927.
43. Castro, C.L., R.A. Pielke & G. Leoncini. 2005. Dynamical downscaling: assessment of value retained and added using the regional atmopsheric modeling system (RAMS). *J. Geophys. Res. D Atmos.* **110:** 1–21.
44. Feser, F., B. Rockel, H. von Storch, *et al.* 2011. Regional climate models add value to global model data: a review and selected examples. *Bull. Am. Meteorol. Soc.* **92:** 1181–1192.
45. Parker, R.J., B.J. Reich & S.R. Sain. 2015. A multiresolution approach to estimating the value added by regional climate models. *J. Clim.* **28:** 8873–8887.
46. Li, D. 2017. Added value of high-resolution regional climate model: selected cases over the Bohai Sea and the Yellow Sea areas. *Int. J. Climatol.* **37:** 169–179.
47. Pfeiffer, A. & G. Zängl. 2011. Regional climate simulations for the European Alpine Region—sensitivity of precipitation to large-scale flow conditions of driving input data. *Theor. Appl. Climatol.* **105:** 325–340.
48. Bard, E., G. Raisbeck, F. Yiou & J. Jouzel. 1999. Solar irradiance during the last 1200 yr based on cosmogenic nuclides. *Tellus B* **52:** 985–992.
49. Schmidt, G.A., J.H. Jungclaus, C.M. Ammann, *et al.* 2011. Climate forcing reconstructions for use in PMIP simulations of the last millennium (v1.0). *Geosci. Model Dev.* **4:** 33–45.
50. Crowley, T.J. & M.B. Unterman. 2013. Technical details concerning development of a 1200 yr proxy index for global volcanism. *Earth Syst. Sci. Data* **5:** 187–197.
51. Sigl, M., M. Winstrup, J.R. McConnell, *et al.* 2015. Timing and climate forcing of volcanic eruptions for the past 2,500 years. *Nature* **523:** 543–549.
52. Toohey, M., B. Stevens, H. Schmidt & C. Timmreck. 2016. Easy Volcanic Aerosol (EVA v1.0): an idealized forcing generator for climate simulations. *Geosci. Model Dev.* **9:** 4049–4070.
53. Pongratz, J., C. Reick, T. Raddatz & M. Claussen. 2008. A reconstruction of global agricultural areas and land cover for the last millennium. *Global Biogeochem. Cycles* **22:** GB3018.
54. Peltier, W.R., D.F. Argus & R. Drummond. 2015. Space geodesy constrains ice age terminal deglaciation: the global ICE-6G-C (VM5a) model. *J. Geophys. Res. Solid Earth* **120:** 450–487.
55. Merz, N., C.C. Raible & T. Woollings. 2015. North Atlantic eddy-driven jet in interglacial and glacial winter climates. *J. Clim.* **28:** 3977–3997.
56. Luterbacher, J., D. Dietrich, E. Xoplaki, *et al.* 2004. European seasonal and annual temperature variability, trends, and extremes since 1500. *Science* **303:** 1499–1503.
57. Pauling, A., J. Luterbacher, C. Casty & H. Wanner. 2006. Five hundred years of gridded high-resolution precipitation

reconstructions over Europe and the connection to large-scale circulation. *Clim. Dyn.* **26:** 387–405.
58. Strandberg, G., E. Kjellström, A. Poska, *et al.* 2014. Regional climate model simulations for Europe at 6 and 0.2 k BP: sensitivity to changes in anthropogenic deforestation. *Clim. Past* **10:** 661–680.
59. Russo, E. & U. Cubasch. 2016. Mid-to-late Holocene temperature evolution and atmospheric dynamics over Europe in regional model simulations. *Clim. Past* **12:** 1645–1662.
60. Mauri, A., B.A.S. Davis, P.M. Collins & J.O. Kaplan. 2015. The climate of Europe during the Holocene: a gridded pollen-based reconstruction and its multi-proxy evaluation. *Quat. Sci. Rev.* **112:** 109–127.
61. Brayshaw, D.J., C.M.C. Rambeau & S.J. Smith. 2011. Changes in Mediterranean climate during the Holocene: insights from global and regional climate modelling. *Holocene* **21:** 15–31.
62. Wanner, H., J. Beer, J. Bütikofer, *et al.* 2008. Mid- to late Holocene climate change: an overview. *Quat. Sci. Rev.* **27:** 1791–1828.
63. Diffenbaugh, N.S., M. Ashfaq, B. Shuman, *et al.* 2006. Summer aridity in the United States: response to mid-Holocene changes in insolation and sea surface temperature. *Geophys. Res. Lett.* **33:** L22712.
64. Patricola, C.M. & K.H. Cook. 2007. Dynamics of the West African monsoon under mid-Holocene precessional forcing: regional climate model simulations. *J. Clim.* **20:** 694–716.
65. Fallah, B., S. Sodoudi, E. Russo, *et al.* 2017. Towards modeling the regional rainfall changes over Iran due to the climate forcing of the past 6000 years. *Quat. Int.* **429:** 119–128.
66. Yu, E., T. Wang, Y. Gao & W. Xiang. 2014. Precipitation pattern of the mid-Holocene simulated by a high-resolution regional climate model. *Adv. Atmos. Sci.* **31:** 962–971.
67. Wagner, S., I. Fast & F. Kaspar. 2012. Comparison of 20th century and pre-industrial climate over South America in regional model simulations. *Clim. Past* **8:** 1599–1620.
68. Paeth, H., C. Steger, J. Li, *et al.* Comparison of Cenozoic surface uplift and glacial–interglacial cycles on Himalaya-Tibet paleo-climate: insights from a regional climate model. *Clim. Past Discuss.* **5194:** 2017–111.
69. Polanski, S., B. Fallah, D.J. Befort, *et al.* 2014. Regional moisture change over India during the past Millennium: a comparison of multi-proxy reconstructions and climate model simulations. *Glob. Planet. Change* **122:** 176–185.
70. Ackerley, D., A. Lorrey, J. Renwick, *et al.* 2013. High-resolution modelling of mid-Holocene New Zealand climate at 6000 yr BP. *Holocene* **23:** 1272–1285.
71. Braconnot, P., S.P. Harrison, M. Kageyama, *et al.* 2012. Evaluation of climate models using palaeoclimatic data. *Nat. Clim. Change* **2:** 417–424.
72. PMIP3 21ka experimental design. Accessed April 18, 2018. https://wiki.lsce.ipsl.fr/pmip3/doku.php/pmip3:des.
73. CLIMAP Project Members; Ruddiman, W.F., R.M.L. Cline, J.D. Hays, *et al.* 1984. The last interglacial ocean. *Quat. Res.* **21:** 123–224.
74. Ray, N. & J.M. Adams. 2001. A GIS-based vegetation map of the world at the last glacial maximum (25,000–15,000 BP). *Internet Archaeol.* **11**. https://archive-ouverte.unige.ch/unige:17817.
75. Bartlein, P.J., S.P. Harrison, S. Brewer, *et al.* 2011. Pollen-based continental climate reconstructions at 6 and 21 ka: a global synthesis. *Clim. Dyn.* **37:** 775–802.
76. Baulin, V.V., N.S. Danilova, V.P. Nechayev, *et al.* 1992. Permafrost: maximum cooling of the last glaciation (about 20,000 to 18,000 yr B.P.). In *Atlas of Paleoclimates and Paleoenvironments of the Northern Hemisphere.* B. Frenzel, M. Pecsi & A.A. Vellchko, Eds. Stuttgart: Gustav Fischer Verlag.
77. Andrieux, E., P. Bertran & K. Saito. 2016. Spatial analysis of the French Pleistocene permafrost by a GIS database. *Permafr. Periglac. Process.* **27:** 17–30.
78. Jost, A., D. Lunt, A. Abe-Ouchi, *et al.* 2005. High-resolution simulations of the last glacial maximum climate over Europe: a solution to discrepancies with continental palaeoclimatic reconstructions? *Clim. Dyn.* **24:** 577–590.
79. Hofer, D., C.C. Raible, A. Dehnert & J. Kuhlemann. 2012. The impact of different glacial boundary conditions on atmospheric dynamics and precipitation in the North Atlantic region. *Clim. Past* **8:** 935–949.
80. Bromwich, D.H., E.R. Toracinta, H. Wej, *et al.* 2004. Polar MM5 simulations of the winter climate of the Laurentide Ice Sheet at the LGM. *J. Clim.* **17:** 3415–3433.
81. Bromwich, D.H., E.R. Toracinta, R.J. Oglesby, *et al.* 2005. LGM summer climate on the southern margin of the Laurentide Ice Sheet: wet or dry? *J. Clim.* **18:** 3317–3338.
82. Muhs, D.R., J.N. Aleinikoff, T.W. Stafford, *et al.* 1999. Late Quaternary loess in northeastern Colorado: part I—age and paleoclimatic significance. *Bull. Geol. Soc. Am.* **111:** 1861–1875.
83. Römer, W., F. Lehmkuhl & F. Sirocko. 2016. Late Pleistocene aeolian dust provenances and wind direction changes reconstructed by heavy mineral analysis of the sediments of the Dehner dry maar (Eifel, Germany). *Glob. Planet. Change* **147:** 25–39.
84. Ju, L., H. Wang & D. Jiang. 2007. Simulation of the Last Glacial Maximum climate over East Asia with a regional climate model nested in a general circulation model. *Palaeogeogr. Palaeoclimatol. Palaeoecol.* **248:** 376–390.
85. Zheng, Y.Q., G. Yu, S.M. Wang, *et al.* 2004. Simulation of paleoclimate over East Asia at 6 ka BP and 21 ka BP by a regional climate model. *Clim. Dyn.* **23:** 513–529.
86. Cook, K.H. & E.K. Vizy. 2006. South American climate during the Last Glacial Maximum: delayed onset of the South American monsoon. *J. Geophys. Res. Atmos.* **111:** D02110.
87. Drost, F., J. Renwick, B. Bhaskaran, *et al.* 2007. A simulation of New Zealand's climate during the Last Glacial Maximum. *Quat. Sci. Rev.* **26:** 2505–2525.
88. Kageyama, M., A. Laîné, A. Abe-Ouchi, *et al.* 2006. Last Glacial Maximum temperatures over the North Atlantic, Europe and western Siberia: a comparison between PMIP models, MARGO sea-surface temperatures and pollen-based reconstructions. *Quat. Sci. Rev.* **25:** 2082–2102.

89. Pfister, C., R. Brázdil, R. Glaser, *et al.* 1999. Documentary evidence on climate in sixteenth-century Europe. *Clim. Change* **43:** 55–110.
90. de Jong, R., S. Björck, L. Björkman & L.B. Clemmensen. 2006. Storminess variation during the last 6500 years as reconstructed from an ombrotrophic peat bog in Halland, southwest Sweden. *J. Quat. Sci.* **21:** 905–919.
91. Winterfeldt, J., B. Geyer & R. Weisse. 2011. Using QuikSCAT in the added value assessment of dynamically downscaled wind speed. *Int. J. Climatol.* **31:** 1028–1039.
92. Somot, S., F. Sevault, M. Déqué & M. Crépon. 2008. 21st century climate change scenario for the Mediterranean using a coupled atmosphere–ocean regional climate model. *Glob. Planet. Change* **63:** 112–126.
93. Drobinski, P., A. Anav, C. Lebeaupin Brossier, *et al.* 2012. Model of the Regional Coupled Earth system (MORCE): application to process and climate studies in vulnerable regions. *Environ. Model. Softw.* **35:** 1–18.
94. Sein, D.V., U. Mikolajewicz, M. Gröger, *et al.* 2015. Regionally coupled atmosphere–ocean–sea ice–marine biogeochemistry model ROM: 1. Description and validation. *J. Adv. Model. Earth Syst.* **7:** 268–304.
95. Ho-Hagemann, H.T.M., M. Gröger, B. Rockel, *et al.* 2017. Effects of air–sea coupling over the North Sea and the Baltic Sea on simulated summer precipitation over Central Europe. *Clim. Dyn.* **49:** 3851–3876.
96. Sein, D.V., N.V. Koldunov, J.G. Pinto & W. Cabos. 2014. Sensitivity of simulated regional Arctic climate to the choice of coupled model domain. *Tellus A Dyn. Meteorol. Oceanogr.* **66:** 23966.
97. Dee, S.G., N.J. Steiger, J. Emile-Geay & G.J. Hakim. 2016. On the utility of proxy system models for estimating climate states over the common era. *J. Adv. Model. Earth Syst.* **8:** 1164–1179.
98. Tolwinski-Ward, S.E., M.N. Evans, M.K. Hughes & K.J. Anchukaitis. 2011. An efficient forward model of the climate controls on interannual variation in tree-ring width. *Clim. Dyn.* **36:** 2419–2439.
99. Christner, E., F. Aemisegger, S. Pfahl, *et al.* 2018. The climatological impacts of continental surface evaporation, rainout, and sub-cloud processes on δ D of water vapor and precipitation in Europe. *J. Geophys. Res. Atmos.* **123:** 4390–4409.
100. Smerdon, J.E., A. Kaplan, E. Zorita, *et al.* 2011. Spatial performance of four climate field reconstruction methods targeting the Common Era. *Geophys. Res. Lett.* **38:** L11705.
101. Matsikaris, A., M. Widmann & J. Jungclaus. 2016. Influence of proxy data uncertainty on data assimilation for the past climate. *Clim. Past* **12:** 1555–1563.
102. Fallah, B., W. Acevedo, E. Russo, *et al.* 2017. Towards high resolution climate reconstruction using an off-line data assimilation and COSMO-CLM 5.00 model. *Clim. Past Discuss.* https://doi.org/10.5194/cp-2017-140.
103. Zängl, G., D. Reinert, P. Rípodas & M. Baldauf. 2015. The ICON (ICOsahedral Non-hydrostatic) modelling framework of DWD and MPI-M: description of the non-hydrostatic dynamical core. *Q. J. R. Meteorol. Soc.* **141:** 563–579.
104. Heinze, R., A. Dipankar, C.C. Henken, *et al.* 2017. Large-eddy simulations over Germany using ICON: a comprehensive evaluation. *Q. J. R. Meteorol. Soc.* **143:** 69–100.
105. Latif, M., M. Claussen, M. Schulz & T. Brücher. 2016. Comprehensive Earth system models of the last glacial cycle. *EoS* **97**. https://eos.org/project-updates/comprehensive-earth-system-models-of-the-last-glacial-cycle.
106. PALEOLINK. Accessed April 18, 2018. http://pastglobalchanges.org/ini/wg/2k-network/pro.
107. Lehner, F., F. Joos, C.C. Raible, *et al.* 2015. Climate and carbon cycle dynamics in a CESM simulation from 850 to 2100 CE. *Earth Syst. Dyn.* **6:** 411–434.
108. V. Ramaswamy, O. Boucher, J. Haigh, *et al.* 2001. Radiative Forcing of Climate Change. In: *Climate Change 2001: The Scientific Basis. Contribution of Working Group I to the Third Assessment Report of the Intergovernmental Panel on Climate Change.* J.T. Houghton, Y. Ding, D.J. Griggs, *et al.*, Eds.: 68. Cambridge, UK and New York, NY: Cambridge University Press.